Angular distribution of Au and Pb *L* x rays following photoionization by synchrotron radiation

H. Yamaoka* and M. Oura
Harima Institute, RIKEN (The Institute of Physical and Chemical Research), 1-1-1 Kouto, Mikazuki, Sayo, Hyogo 679-5148, Japan

K. Takahiro, N. Takeshima, and K. Kawatsura
Kyoto Institute of Technology, Matsugasaki, Sakyo, Kyoto 606-8585, Japan

M. Mizumaki
Japan Synchrotron Radiation Research Institute (JASRI), 1-1-1 Kouto, Mikazuki, Sayo, Hyogo 679-5198, Japan

U. Kleiman
Institut für Theoretische Physik, Westfälische Wilhelms-Universität Münster, Wilhelm-Klemm-Strasse 9, D-48149 Münster, Germany

N. M. Kabachnik†
Fakultät für Physik, Universität Bielefeld, D-33615 Bielefeld, Germany

T. Mukoyama
Kansai Gaidai University, 16-1 Nakamiyahigashino, Hirakata, Osaka 573-1001, Japan
(Received 31 January 2002; published 14 June 2002)

Angular distribution of L x rays of Au and Pb following photoionization by synchrotron radiation has been measured at the incident photon energies corresponding to the energy between L_3 and L_2, between L_2 and L_1, and above L_1 absorption edges. No evidence of L x-ray anisotropy was observed within the experimental errors for all incident photon energies, but in the case of L_l x rays an anisotropy of a few percent might be possible. The experimental results are in good agreement with the theoretical prediction.

DOI: 10.1103/PhysRevA.65.062713 PACS number(s): 32.80.Fb, 32.30.Rj, 34.10.+x

I. INTRODUCTION

Ionization of atoms by electrons, high-velocity ions, and photons leads to the alignment of inner-shell vacancy with the total angular momentum $J>1/2$ because the magnetic sublevels of the resulting ion have a nonstatistical population. The alignment effect can be measured by the nonisotropic angular distribution of the emitted Auger electrons and x rays, or by the partial polarization of the emitted photons. This phenomenon was theoretically predicted by Mehlhorn [1], Flügge *et al.* [2], and Jacobs [3]. Extensive studies for the L_3 subshell have been performed by heavy-ion bombardments [4–12] and by electron-impact ionization [13–17]. These experimental data are in good agreement with the theoretical calculations [18–20]. The alignment effect is considered to be well established for electron impact [21] and in ion-atom collisions [22].

However, two effects should be taken into account to interpret these experimental data. First, these data are obtained for all of the subshells including the ones with $J=1/2$, which have no alignment effect. The Coster-Kronig transitions from these states to the state with $J>1/2$ reduce the alignment effect, and the atomic parameters, such as subshell ionization cross sections, Coster-Kronig probabilities, and subshell fluorescence yields, are necessary to estimate the alignment effect [8]. Second, multiple ionization commonly occurs in the process of ionization by heavy ions.

On the other hand, the study of the alignment induced by photoionization has the advantage of negligible multiple-ionization effect. In addition, it is possible to ionize the subshell of interest by tuning the energy of the incident x rays and to avoid the alignment dilution effect inherent to the Coster-Kronig process. Considering these facts, the study of the alignment of ionized atoms following photoionization is useful to test the theoretical predictions. First theoretical studies [23–25] have shown, that the alignment produced in photoionization and, therefore, the angular anisotropy of x rays and Auger electrons, may be large near the ionization threshold, in the region of the Cooper minimum and in the far relativistic region ($E>1$ MeV). On the other hand, at the photon energies corresponding to the fast but still nonrelativistic photoelectrons ($E_e \approx 1-100$ keV) the predicted alignment is small, typically less than 10%.

The experimental investigation of the alignment resulting from photoionization has been performed using He I radiation by Caldwell and Zare [26]. Later the synchrotron radiation was used for studying the alignment of inner-shell vacancies in medium-weight atoms by means of fluorescence spectroscopy in Cd($4d^{-1}$) [27] and by means of Auger-electron spectroscopy in Mg($2p^{-1}$) [28], Kr($3d^{-1}$) [29], and Xe($4d^{-1}$) [30–32]. The majority of the cited papers showed a good agreement between the experimental results and the theoretical calculations. Recently, Schmoranzer and coworkers [33–37] have used the photon-induced fluorescence spectroscopy (PIFS) in the vacuum ultraviolet (VUV)

*Electronic address: yamaoka@spring8.or.jp
†Also at Institute of Nuclear Physics, Moscow State University, Moscow 119899, Russia.

region with synchrotron wiggler radiation at the BESSY storage ring (Berlin) for studying the alignment in Kr II, Xe II and Ar II. Meyer *et al.* [38] measured the alignment of Xe ions in the resonant Auger decay induced by photoexcitation at the Super-ACO storage ring in Orsay. With these experimental results the effect of the alignment was found in the case of PIFS in the VUV region. Here also the experimental results are basically in agreement with the theoretical calculations [36,38].

However, the experimental results for the angular distributions of L x rays from heavy elements are contradictory. Kahlon *et al.* [39,40] and Sharma and Allawadhi [41] reported strong anisotropy of L x-ray emission from Th, U, and Au. Ertuğrul and co-workers [42–44] and Seven and Koçak [45] showed results similar to those of Kahlon *et al.* for L x rays from a range of heavy atoms $70 \leqslant Z \leqslant 92$. The anisotropy they observed is much larger than the theoretical values of Oh and Pratt [23], Scofield [24], and Berezhko *et al.* [25]. On the other hand, Kumar *et al.* [46,48] and Mehta and coworkers [47] reported an isotropic emission of L x rays for Pb, Th, and U within experimental errors. Those four groups used radioisotopes (RI) as photon sources or secondary sources excited by RI sources. Papp and Campbell [49] used an x-ray generator as the photon source and showed that the largest anisotropy of Er L_l emission was about 4%. This result is slightly higher than the theoretical prediction [25]. It is interesting to measure the angular distributions of L x rays more precisely and to elucidate the discrepancy among the previous experimental data. For this purpose, it is advantageous to use the third-generation synchrotron radiation facility and to excite each L subshell selectively. Such experiments have not been performed so far.

In this paper we report the experimental results for L x-ray emission from Au and Pb following photoionization by synchrotron undulator radiation at the SPring-8 storage ring. In order to compare the experimental results with theory, we have calculated the alignment using the Hartree-Fock approximation. The largest anisotropy is expected when the excitation energy is tuned between the L_2- and L_3-subshell ionization thresholds because only the L_3 subshell is ionized and there is no contamination from the Coster-Kronig transitions. In addition, we changed the incident photon energies to the values between L_2 and L_1, and above L_1 absorption edges, in order to study the effect of the Coster-Kronig processes on the alignment of the L_3 state. Au and Pb targets were chosen for a direct comparison with the previous experiments described above.

II. THEORY

The angular distribution of the fluorescence radiation emitted after ionization of an atom by linearly polarized photons is described by the well-known equation [18,50]

$$\frac{dI}{d\Omega} = \frac{I_0}{4\pi}[1 + \beta P_2(\cos\theta)], \tag{1}$$

where $P_2(\cos\theta)$ is the second Legendre polynomial, θ is the angle between the electric-field vector of the exciting radiation and the direction of propagation of the fluorescence radiation, I_0 is the total fluorescence intensity integrated over all angles, and Ω is the solid angle. Equation (1) shows an axially symmetric angular distribution with respect to the electric vector of the incident photon beam. The anisotropy parameter β is a product of the kinematic term α and the alignment $\mathcal{A}_{20}$ of the initial state populated by the linearly polarized light [18],

$$\beta = \alpha \mathcal{A}_{20}(J_1), \tag{2}$$

where α is calculated according to

$$\alpha = \sqrt{\frac{3}{2}(2J_1+1)}(-1)^{J_1+J_2+1}\begin{Bmatrix} 1 & J_1 & J_2 \\ J_1 & 1 & 2 \end{Bmatrix}. \tag{3}$$

Here J_1 and J_2 are the angular momenta of the initial and final states, respectively, and the standard notation for the $6j$ symbol is used. The values of α are 1/10, $-2/5$, 1/10, $-2/5$, 1/10, 1/2, $-2/5$, and 1/2 for the emissions of $L_{\alpha 1}$ (L_3-M_5), $L_{\alpha 2}$ (L_3-M_4), $L_{\beta 2}$ (L_3-N_5), $L_{\beta 5}$ (L_3-O_4), $L_{\beta 5}$ (L_3-O_5), $L_{\beta 6}$ (L_3-N_1), $L_{\beta 15}$ (L_3-N_4), and L_l (L_3-M_1) x-rays, respectively. On the other hand, these values are 0 for the other x-ray emissions, L_η (L_2-M_1), $L_{\beta 1}$ (L_2-M_4), $L_{\beta 3}$ (L_1-M_3), $L_{\beta 4}$ (L_1-M_2), $L_{\gamma 1}$ (L_2-N_4), $L_{\gamma 3}$ (L_1-N_3), $L_{\gamma 4}$ $(L_1-O_{2,3})$, and $L_{\gamma 6}$ (L_2-O_4), related to the L_2 and L_1 subshells because the initial angular momentum is $J_1=1/2$ for these transitions and such states cannot be aligned [18]. Since the L_α $(= L_{\alpha 1} + L_{\alpha 2})$ lines were not resolved in the present experiment, the average value of α weighted by the calculated emission rates [51] is estimated to be about 0.049 for both Au and Pb. Thus, the anisotropy of the L_α line is expected to be small. The largest anisotropy is expected for the L_l and $L_{\beta 6}$ lines. When the vacancy is produced in the L_1 and L_2 shells, we have to take into consideration the Coster-Kronig processes too.

The degree of alignment $\mathcal{A}_{20}(J_1)$ for a state with $J_1 = 3/2$ is simply defined by

$$\mathcal{A}_{20}(3/2) = \frac{\sigma_{3/2} - \sigma_{1/2}}{\sigma_{3/2} + \sigma_{1/2}}, \tag{4}$$

where $\sigma_{3/2}$ and $\sigma_{1/2}$ are the total photoionization cross sections for the magnetic substates $m_j = 3/2$ and 1/2, respectively [18]. In Sec. IV we present the results of our calculations of the degree of alignment. The calculations were made within the independent electron model. Though the considered atoms Au and Pb are open-shell atoms, the interaction of the valence electrons with the deep inner $2p_{3/2}$ vacancy is very weak and can be ignored. Thus the alignment of the $2p_{3/2}^{-1}$ state may be considered as in a closed-shell atom. Within this approximation the general expression for $\mathcal{A}_{20}$ can be written as

$$\mathcal{A}_{20}(J_1) = \frac{\Sigma_{l,j} b(j,J_1) |D_{\varepsilon lj}|^2}{\Sigma_{l,j} |D_{\varepsilon lj}|^2}, \tag{5}$$

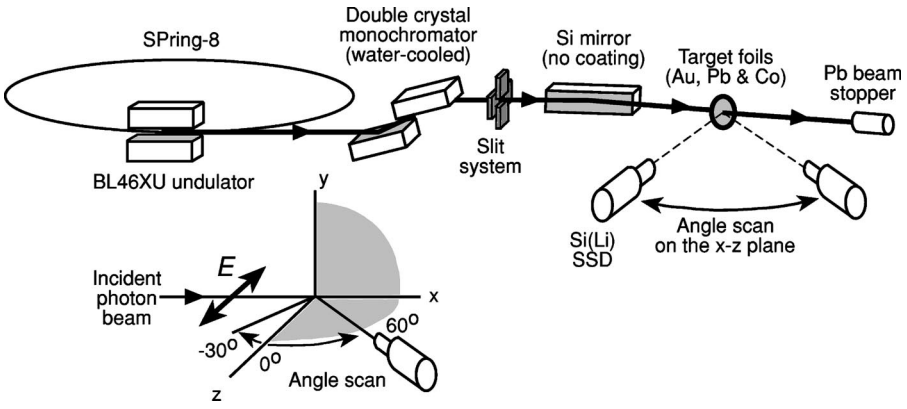

FIG. 1. Schematic diagram of the experimental setup and coordinate system. Angle scan was performed in the *x*-*z* plane. The incident photon beam was the linearly polarized undulator radiation.

$$b(j,J_1)=(-1)^{j+J_1}\sqrt{6(2J_1+1)}\begin{Bmatrix}2 & 1 & 1\\ j & J_1 & J_1\end{Bmatrix}, \qquad (6)$$

where $D_{\varepsilon lj}$ is the dipole ionization amplitude, corresponding to the emission of a photoelectron with the (orbital) total angular momentum $(l)j$ [50]. The dipole ionization amplitudes may be reduced to the single electron matrix elements and then to the radial dipole integrals, so that the alignment of a vacancy in the $2p_{3/2}$ subshell may be written as [25,52]

$$\mathcal{A}_{20}(2p_{3/2})=-\frac{R^2_{\varepsilon s,2p}+\frac{1}{5}R^2_{\varepsilon d,2p}}{R^2_{\varepsilon s,2p}+2\,R^2_{\varepsilon d,2p}}, \qquad (7)$$

where

$$R_{\varepsilon s(d),2p}=\int_0^\infty dr\, P_{\varepsilon s(d)}(r) r P_{2p}(r) \qquad (8)$$

are the single-particle radial dipole integrals (length form); $P_{2p}(r)$ denotes the radial wave function of the bound electron while $P_{\varepsilon s(d)}(r)$ are the radial wave functions of the ejected photoelectron; the spin-orbit interaction in the continuum is neglected [61].

The radial dipole integrals (8) have been evaluated by applying a relaxed orbital method within a single-configuration Hartree-Fock approach [53], that is, the bound-electron wave function $P_{2p}(r)$ has been calculated in the field of the atom whereas the continuum electron wave functions $P_{\varepsilon s(d)}(r)$ have been obtained in the field of the singly ionized atom. In addition, mass-velocity and Darwin corrections have been incorporated within the format of the nonrelativistic Hartree-Fock approach (Hartree-Fock-Roothaan method) [53,54].

Here we note that the calculations have been done in the dipole approximation. In the considered photon energy range (1–50 keV) the contribution of quadrupole photoabsorption may be significant. Analysis of the nondipolar effects made by Kabachnik and Sazhina [55] has shown that the most important electric-quadrupole interaction can lead to an additional alignment and also to the axial asymmetry with respect to the electric vector. However, as follows from the relativistic calculations [23,24,55], both effects are small, less than 2% at the considered energies.

It is also noted that in the case of unpolarized incident light the bracket on the right side of Eq. (1) is written as $1-(\beta/2)P_2(\cos\theta)$, where θ is the angle with respect to the beam direction (x axis in Fig. 1). Therefore, the alignment effect will be enhanced for the polarized beam compared to the case when the unpolarized beam is used.

III. EXPERIMENT AND ANALYZING PROCEDURE

Figure 1 shows the experimental setup and the coordinate system. The experiment was carried out at the undulator beamline BL46XU of the SPring-8 storage ring. The undulator radiation was monochromatized by the fixed-exit and water-cooled Si double crystal monochromator. The incident photon beam was linearly polarized synchrotron radiation ($P_{lin}\geqslant 99\%$) with the electric vector in the horizontal direction which is chosen to be the z axis of our coordinate system, as shown in Fig. 1. The linear polarization was confirmed in the similar beam line BL39XU at the SPring-8 by x-ray magnetic diffraction experiment [56]. In front of the target we placed a Si mirror without any coating materials to prevent higher-order diffraction from the monochromator.

Self-supporting target of pure Au, Pb, and Co 0.25-μm-thick micro foils (483, 266.7, and 94.6 μg/cm^2, respectively) evaporated on Mylar or Acrylic backing were used. Such thin foils reduce the factor of the intensity correction in the absorption of the incident beam and the emitted photons for the measured raw data. Co K x rays were used as a monitor of the incident beam intensity. The size of the incident photon beam was adjusted by a slit system on the beamline. The maximum beam footprint on the target was about 1.0 mm in height and 2.9 mm in width, corresponding to about 10% of the detector area (active diameter of 6 mm). The detector was a Si(Li) solid-state detector (SSD) (SEIKO EG & G SLP-06180-P) with full width at half maximum of 167 eV at 5.9 keV (catalogue value). The target and the detector were set on a Huber 5020 eight-axis diffractometer.

The detector angle scan was performed in the x-z plane. The sample angle was fixed. The scanning angle was measured with respect to the direction of the electric vector of the incident photon beam, as shown in Fig. 1. When the SSD is placed in the direction of the electric vector (z axis in Fig. 1), the angle corresponds to 0°. The sample angle with respect to the incident photon beam was corrected by setting ionization chambers just before and after the target and by

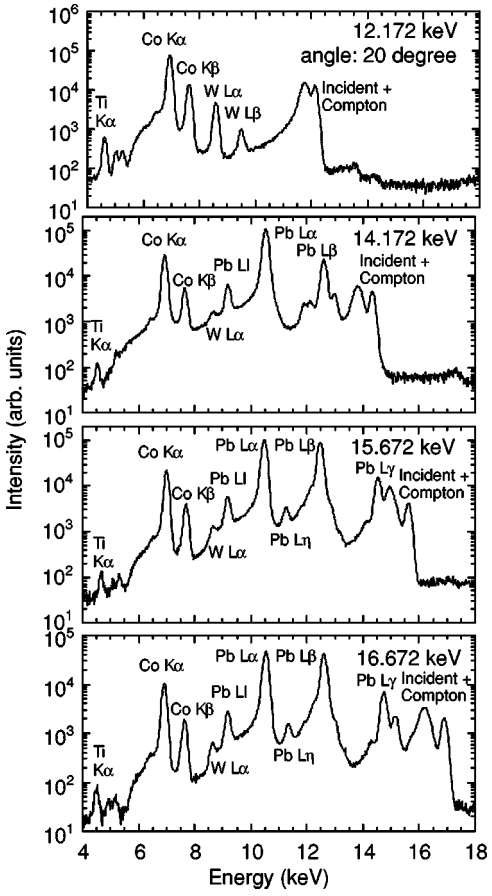

FIG. 2. Example of the Pb L x-ray spectra for the incident photon energies of 12.172, 14.172, 15.672, and 16.672 keV measured at an angle of 20°. At 12.172 keV, below L_3 absorption edge, no Pb L x rays were observed.

measuring the change in the incident photon intensity while the sample angle was changed. The incident photon energy was corrected by using the Au L absorption edges of a 50-μm-thick foil. The angular distribution of L x rays were measured at every 5° in the detector angle range from $-30°$ to 60°. The incident photon energies were chosen to be 13.172, 14.172, and 15.172 keV for the Au target, and 14.172, 15.672, and 16.672 keV for the Pb target.

According to the theoretical prediction, the expected anisotropy is small. The largest anisotropy is expected for the L_l or $L_{\beta 6}$ lines [18], whose intensity is, however, much weaker than that of the lines like L_α or L_β. Considering these facts, total counts larger than 10^4 for the L_l line were accumulated to obtain statistical error smaller than 1% at every angle.

Typical spectra of Pb L and Co K x rays at four incident energies at an angle of 20° are shown in Fig. 2. Two small peaks above the Co K lines may originate from the fluorescence of the tungsten slit system, but they have little influence on the nearest L x-ray peak, the L_l line. Below the L_3 absorption edge (12.172 keV), no Pb L x rays were observed. There were also no L x-ray lines from Pb when we took off the target at 16.672 keV. We had to confirm this especially for the Pb target because the measurement system, including

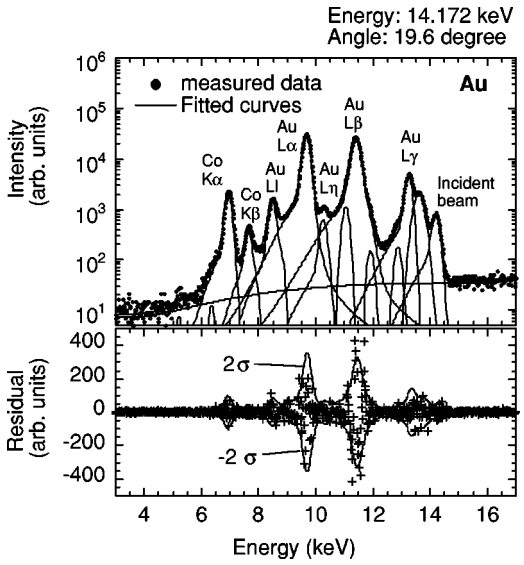

FIG. 3. Upper part of the panel: an example of the experimental data (small closed circle) and fitted curves (solid lines) for Au L x-ray emission at the incident photon energy of 14.172 keV and at the angle of 19.6°. Lower part of the panel: residuals of the fitted curve and the experimental data.

the Si mirror, was inside the monochromatic beam hutch, made of iron/lead/iron x-ray shields, and the detector and the mirror were also covered by lead shields.

Figure 3 shows an example of the experimental spectra, fitted curves and residuals between the experimental data and the fitted curve for the Au target at an incident energy of 14.172 keV and a detection angle of 19.6°. The spectra were analyzed by a least-squares fitting with a nearly Gaussian function for each peak and a polynomial function for the background. The least-square deviation, χ squares, was, for example, about 1.4 for the data in Fig. 3. Since we used the Si(Li) SSD, each line in the spectrum had a low-energy tail. We took into account the tail component as the response function in the fitting [57,58]. A systematic fitting procedure was used for all the spectra at a given incident energy and thus the relative error of the line intensity for the change in the detector angle became small. As described before, the statistical error was less than 1%. The main contribution to the error came from the fitting error. This error was estimated from the square root of the sum of the residuals (between the experimental data and the fitted curve for each line) squared. The total error was, for example, about $\pm 5-6$ % for the L_l line. The line intensities were corrected for the effects of absorption such as the incident-beam attenuation, self-absorption of the emitted x rays, absorption by air between the sample and the detector [59,60]. The relative difference of the self-absorption correction for the change in the detector angle was less than about 1% because we used thin foils. Attenuation of the emitted photons was mainly caused by the air between the sample and the detector. But this effect was the same for any scanned angle. We assumed the SSD efficiency to be 100% in the measured energy range of about 7–17 keV.

TABLE I. Comparison of the measured L x-ray emission rates (normalized to unity) for the L_3 subshells of Au and Pb with the theoretical values by Scofield [51]. The average values taken over all the studied angles are used.

Shell	Line	Experiment	Theoretical
Au L_3	L_l	0.0462 ± 0.0026	0.0396
	L_α	0.7747 ± 0.0134	0.7881
	L_β	0.1791 ± 0.0065	0.1723
Pb L_3	L_l	0.0449 ± 0.0012	0.0411
	L_α	0.7706 ± 0.0207	0.7792
	L_β	0.1844 ± 0.0104	0.1798

IV. RESULTS AND DISCUSSION

In Table I we compare the experimental L x-ray emission rates for Au and Pb L_3 subshell, normalized to unity for each subshell, with the theoretical values of Scofield [51], which have been widely used. The average values taken over all the angles were used. One can see that our experimental results agree well with the theoretical values. Figures 4 and 5 show the results of the angular dependence of Au L x rays at the incident photon energies of 13.172, 14.172, and 15.172 keV. Similar results for Pb L x rays at the incident photon energies of 14.172, 15.672, and 16.672 keV are shown in Figs. 6 and 7. The solid lines correspond to the average values. Here the L_γ line intensities are not shown because they were on the Compton profile of the incident photon beam and the separation was not sufficiently good, especially at the energies between L_2 and L_1 absorption edges. As seen in Figs. 5 and 7 the experimental errors for the L_l and L_η lines are larger than for others because their intensities are low and they are located on the strong low-energy tail of the L_α and L_β lines, respectively.

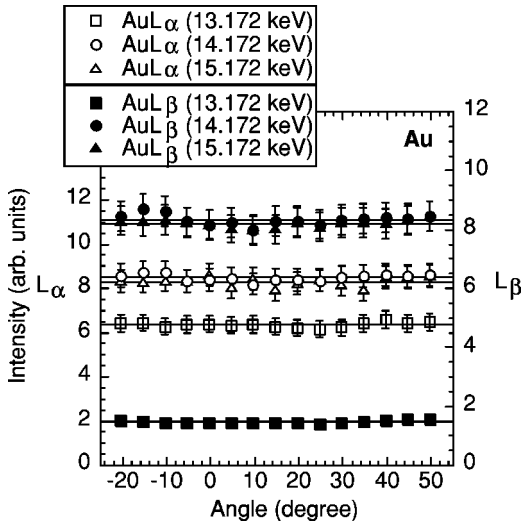

FIG. 4. Angular dependence of the Au L_α and L_β lines at the incident photon energies of 13.172, 14.172, and 15.172 keV. Solid lines show the average values taken over all the angles. Angle was measured from the direction of the electric-field vector of the incident photon beam as shown in Fig. 1.

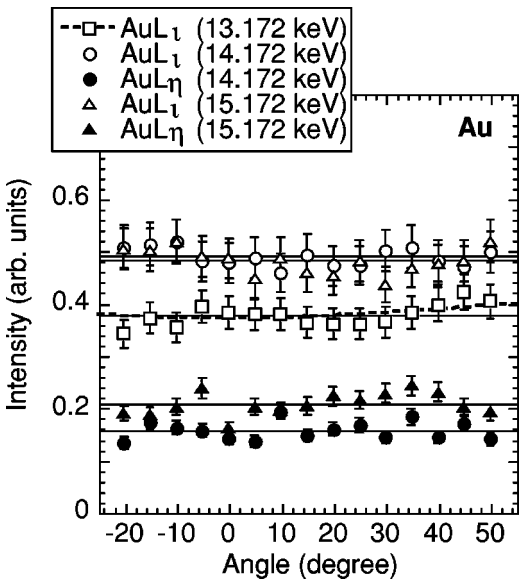

FIG. 5. The same as in Fig. 4 but for the Au L_l and L_η lines. The dashed line shows theoretically calculated curve for L_l line at 13.172 keV according to Eq. (1).

It is clear from Figs. 4–7 that the emission of all of the L x rays studied in the present work, i.e. L_α, L_β, L_η, and L_l rays, is isotropic within experimental errors of a few percent for all incident photon energies used in the experiment. However, due to the experimental errors we cannot exclude the possibility in which there is a weak angular dependence for L_l x rays. Even in this case the anisotropy is about a few percent. The present results contradict the previous experimental data for Au by Kahlon *et al.* [40] and by Ertuğrul and

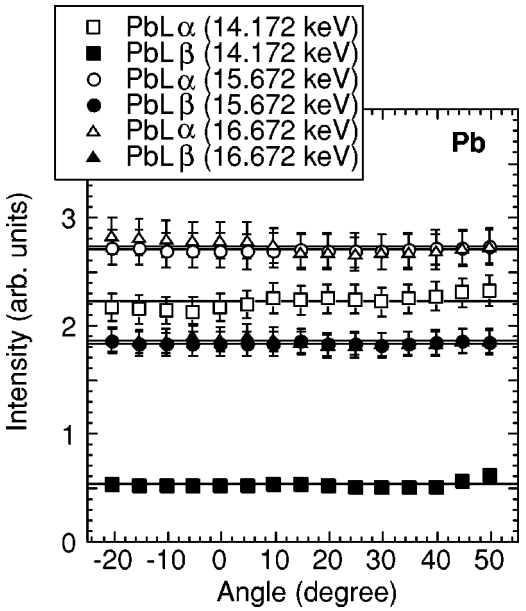

FIG. 6. Angular dependence of the Pb L_α and L_β lines at the incident photon energies of 14.172, 15.672, and 16.672 keV. Solid lines show the average values taken over all the angles.

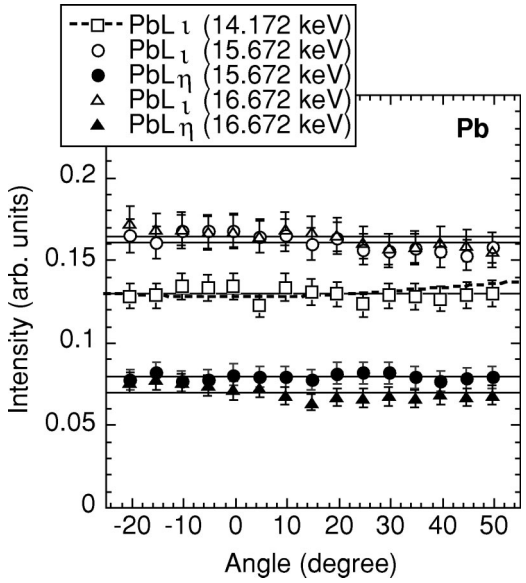

FIG. 7. The same as in Fig. 6 but for the Pb L_l and L_η lines. The dashed line shows theoretically calculated curve for L_l line at 14.172 keV according to Eq. (1).

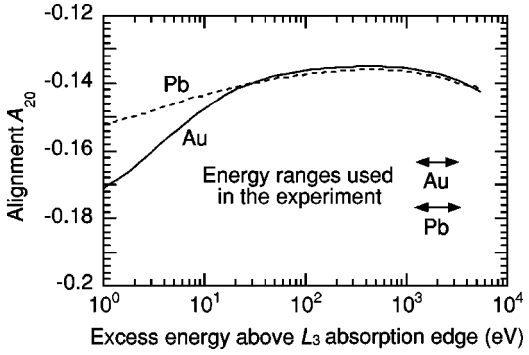

FIG. 8. The calculated alignment $\mathcal{A}_{20}$ as a function of the energy above the L_3 threshold for Au and Pb. The photon energy ranges used in the experiment are also shown. Note that $\mathcal{A}_{20}$ is almost constant (-0.14) for both elements in the energy range used in our experiments.

co-workers [42,43] and for Pb by Ertuğrul [43]. They measured the angular distribution of L x rays induced by 59.57-keV γ rays from ^{241}Am with Si(Li) detectors. No angular dependence was found for the L_β and L_γ x rays, but they observed a strong anisotropy for the L_α and L_l lines. They also claimed the existence of an extra $P_1(\cos\theta)$ term in Eq. (1), which means axial asymmetry.

On the other hand, our measurements are in agreement with the experimental results of Kumar *et al.* for Pb [46] as well as for other heavy atoms [47]. They performed experiments similar to Kahlon *et al.* [40] and Ertuğrul and coworkers [42,43], but found that the angular distribution of all the L x rays is isotropic within the experimental errors. Our result is also consistent with the small anisotropy for the L_α and L_l lines observed by Papp and Campbell [49] who also did not find any contribution of the $P_1(\cos\theta)$ term.

Recently two groups [41,48] measured the angular distributions of L x rays using selective photoionization of L_3 subshell. As discussed above, there is no Coster-Kronig transitions after L_3-subshell photoionization and the emission of the L_l x rays has a larger anisotropy. The incident x rays with an energy between the L_3 and L_2 absorption edges were produced with converters made of suitable elements excited by ^{241}Amγ rays. Although both groups used similar experimental procedures, their conclusion was completely opposite. Sharma and Allawadhi [41] investigated the L_l, L_α, and L_β lines in Th and U and found an anisotropic emission for all the L x rays. The reason for the anisotropy of the L_β x rays was ascribed to the selective excitation of the L_3 shell. On the other hand, Kumar *et al.* [48] measured the angular distributions of the L_l, L_α, and $L_{\beta 2,5,6,7,15}$ x rays for Pb, Th, and U. Their experimental results indicate that the differential cross sections for all the L x rays are angle independent within their experimental errors.

In the present experiment, emission of the L_α, L_β, L_l, and L_η lines is isotropic within the experimental errors for all excitation energies. This means that even when the incident photon energy is between the L_3 and L_2 absorption edges, where the largest anisotropy is expected, no evidence of the anisotropy was observed. The present result is in agreement with that of Kumar *et al.* [48] and indicates that in the present measurements it is not possible to study the alignment including the effect of the Coster-Kronig transitions on the anisotropy of x rays as performed by Kamiya *et al.* [8].

In order to compare the experimental results with the theoretical predictions, we calculated the degree of the alignment above the L_3 absorption edge as a function of the photoelectron energy by using the Hartree-Fock method (see Sec. II). The obtained results for Au and Pb are shown in Fig. 8 with the used energy region in the experiment. The calculated values depend on the photoelectron energy in the energy region below 10 eV, near to the L_3 ionization threshold. But there is almost no energy dependence in the energy region far from the threshold, where we did the experiments, and the value of the alignment $\mathcal{A}_{20}$ is about -0.14. As calculated in Sec. II, the values of α are 1/2 for the L_l and $L_{\beta 6}$ lines, and 0.049 for the L_α line. Thus the anisotropy is estimated to be -0.07 for the L_l and $L_{\beta 6}$ lines, and -0.007 for the L_α line. In Figs. 5 and 7 the calculated curves (the dashed lines) for L_l line at 13.172 keV for Au and at 14.172 keV for Pb are shown. The measured angular dependence of the x-ray emission shows that an anisotropy of a few percent might be possible for the L_l lines. Thus the results of the calculations agree with our experimental results.

Here we did not calculate the anisotropy parameter according to Eq. (1) from the measured data because the errors are still too large to evaluate accurately such small anisotropy. Experimentally we cannot resolve the $L_{\beta 6}$ emission clearly and the L_l and $L_{\beta 6}$ lines are on the large low-energy tails (the response functions) of L_α and L_β, respectively. Even by accumulating data for a longer time and thus reducing further the statistical error, the problems of the resolution

and the response function of the detector still remain as long as a SSD is used. It is not easy to evaluate such a small anisotropy experimentally and the theory still remains to be fully tested. To measure a small anisotropy more accurately, one needs to use a crystal spectrometer instead of a SSD to separate each line.

V. CONCLUSION

The angular distribution of L x rays from Au and Pb following photoionization were measured. The L subshells were selectively ionized by using the synchrotron undulator radiation. For all incident photon energies studied, our experimental results show no evidence of anisotropy for the L x rays from Au and Pb within the experimental errors, but for L_l x rays there might be small anisotropy of about a few percent-.The results are in agreement with the experimental data of Papp and Campbell [49] and Kumar *et al.* [46–48], but contradict those of Kahlon *et al.* [39,40] and Sharma and Allawadhi [41] and of Ertuğrul and co-workers [42–44]. The present experimental results agree with the theoretical calculations based on the Hartree-Fock method. Because of the very small anisotropy, we could not study the effect of the Coster-Kronig transitions on the L_3-subshell alignment.

To determine the value of the anisotropy parameters more exactly, it is necessary to measure the emission lines with a higher energy resolution by using a crystal spectrometer. Then we might be able to test the theory more precisely and also to detect the effect of the Coster-Kronig processes on the alignment.

ACKNOWLEDGMENTS

We thank Dr. N. Akao of Tottori University for the help with the experiment, and Professor C. Itoh of Wakayama University and A. Tamura of SEIKO EG & G for kindly lending us the Si(Li) SSD. We are grateful to Dr. S. Goto of JASRI and Dr. T. Papp of ATOMKI for the advice about the response function of the SSD. N.M.K. is grateful to the Bielefeld University for hospitality and to the Deutsche Forschungsgemeinschaft (DFG) for the financial support within the Mercator professorship program. The experiments were performed at the SPring-8 with the approval of the Japan Synchrotron Radiation Research Institute (JASRI) under the proposal numbers 2000B0089-NS-np and 2001A0107-NS-np.

[1] W. Mehlhorn, Phys. Lett. **26A**, 166 (1968).
[2] S. Flügge, W. Mehlhorn, and V. Schmidt, Phys. Rev. Lett. **29**, 7 (1972).
[3] V.L. Jacobs, J. Phys. B **5**, 2257 (1972).
[4] K.A. Jamison and P. Richard, Phys. Rev. Lett. **38**, 484 (1977).
[5] E.H. Pederson, S. Stephen, J. Czuchlewski, M.D. Brown, L.D. Ellsworth, and J.R. Macdonald, Phys. Rev. A **11**, 1267 (1975).
[6] A. Schöler and F. Bell, Z. Phys. A **286**, 163 (1978).
[7] W. Jitschin, H. Kleinpoppen, R. Hippler, and H.O. Lutz, J. Phys. B **12**, 4077 (1979); W. Jitschin, R. Hippler, R. Shanker, H. Kleinpoppen, R. Schuch, and H.O. Lutz, *ibid.* **16**, 1417 (1983).
[8] M. Kamiya, Y. Kinefuchi, H. Endo, A. Kuwako, K. Ishii, and S. Morita, Phys. Rev. A **20**, 1820 (1979).
[9] A. Hitachi, Y. Awaya, T. Kambara, Y. Kanai, M. Kase, H. Kumagai, J. Takahashi, T. Mizokawa, and A. Yagishita, J. Phys. B **24**, 3009 (1991); T. Papp, Y. Awaya, A. Hitachi, T. Kambara, Y. Kanai, T. Mizokawa, and I. Török, *ibid.* **24**, 3797 (1991).
[10] T. Papp, J.L. Campbell, and J.A. Maxwell, Phys. Rev. A **48**, 3062 (1993).
[11] R. Döner, K. Ullmann, J. Euler, R. Koch, I. Egrand, R. Seip, J. Ullrich, and H. Schmidt-Böcking, J. Phys. B **26**, 3559 (1993).
[12] V.P. Petukhov, E.A. Romanovsky, and H. Kerkow, Nucl. Instrum. Methods Phys. Res. B **109/110**, 19 (1996).
[13] J. Hrdý, A. Henins, and J.A. Bearden, Phys. Rev. A **2**, 1708 (1970).
[14] B. Cleff and W. Mehlhorn, J. Phys. B **7**, 593 (1974); **7**, 605 (1974).
[15] W. Weber, R. Huster, M. Kamm, and W. Mehlhorn, Z. Phys. D: At., Mol. Clusters **22**, 419 (1991).
[16] B. Borucki, W. Weber, and W. Mehlhorn, J. Phys. B **26**, L197 (1993).
[17] H. Küst and W. Mehlhorn, J. Phys. B **34**, 4155 (2001).
[18] E.G. Berezhko and N.M. Kabachnik, J. Phys. B **10**, 2467 (1977).
[19] E.G. Berezhko, N.M. Kabachnik, and V.V. Sizov, J. Phys. B **11**, 1819 (1978).
[20] F. Rösel, D. Trautmann, and G. Bauer, Z. Phys. A **304**, 75 (1982).
[21] W. Mehlhorn, Nucl. Instrum. Methods Phys. Res. B **87**, 227 (1994).
[22] M. Benhenni, S.M. Shafroth, and J.K. Swenson, Nucl. Instrum. Methods Phys. Res. B **86**, 28 (1994).
[23] S.D. Oh and R.H. Pratt, Phys. Rev. A **10**, 1198 (1974).
[24] J.H. Scofield, Phys. Rev. A **14**, 1418 (1976).
[25] E.G. Berezhko, N.M. Kabachnik, and V.S. Rostovsky, J. Phys. B **11**, 1749 (1978).
[26] C.D. Caldwell and R.N. Zare, Phys. Rev. A **16**, 255 (1977).
[27] W. Kronast, R. Huster, and W. Mehlhorn, J. Phys. B **17**, L51 (1984); Z. Phys. D: At., Mol. Clusters **2**, 285 (1986).
[28] B. Kämmerling, A. Hausmann, J. Lüger, and V. Schmidt, J. Phys. B **25**, 4773 (1992).
[29] B. Kämmerling, B. Krässig, O. Schwarzkopf, J.P. Ribeiro, and V. Schmidt, J. Phys. B **25**, L5 (1992).
[30] S.H. Southworth, P.H. Kobrin, C.M. Truesdale, D. Lindle, S. Owaki, and D.A. Shirley, Phys. Rev. A **24**, 2257 (1981); S. Southworth, U. Becker, C.M. Truesdale, P.H. Kobrin, D.W. Lindle, S. Owaki, and D.A. Shirley, *ibid.* **28**, 261 (1983).
[31] S.B. Whitfield, C.D. Caldwell, D.X. Huang, and M.O. Krause, J. Phys. B **25**, 4755 (1992).
[32] G. Snell, E. Kukk, B. Langer, and N. Berrah, Phys. Rev. A **61**, 042709 (2000).
[33] H. Schmoranzer, S. Lauer, F. Vollweiler, A. Ehresmann, V.L. Sukhorukov, B.M. Lagutin, I.D. Petrov, Ph.V. Demekhin,

K.-H. Schartner, B. Magel, and G. Mentzel, J. Phys. B **30**, 4463 (1997).
[34] G. Metzel, K.-H. Schartner, O. Wilhelmi, B. Magel, U. Staude, F. Vollweiler, S. Lauer, H. Leibel, H. Schmoranzer, V.L. Sukhorukov, and B.M. Lagutin, J. Phys. B **31**, 227 (1998).
[35] A. Ehresmann, H. Schäffer, F. Vollweiler, G. Mentzel, B. Magel, K.-H. Schartner, and H. Schmoranzer, J. Phys. B **31**, 1487 (1998).
[36] B.M. Lagutin, I.D. Perov, Ph.V. Demekhin, V.L. Sukhorukov, F. Vollweiler, H. Liebel, A. Ehresmann, S. Lauer, H. Schmoranzer, O. Wilhelmi, B. Zimmermann, and K.-H. Schartner, J. Phys. B **33**, 1337 (2000).
[37] B. Zimmermann, O. Wilhelmi, K.-H. Schartner, F. Vollweiler, H. Liebel, A. Ehresmann, S. Lauer, H. Schmoranzer, B.M. Lagutin, I.D. Petrov, and V.L. Sukhorukov, J. Phys. B **33**, 2467 (2000).
[38] M. Meyer, A. Marquette, A.N. Grum-Grzhimailo, U. Kleiman, and B. Lohmann, Phys. Rev. A **64**, 022703 (2001).
[39] K.S. Kahlon, H.S. Aulakh, N. Singh, R. Mittal, K.L. Allawadhi, and B.S. Sood, J. Phys. B **23**, 2733 (1990); K.S. Kahlon, H.S. Aulakh, N. Singh, R. Mittal, K.L. Allawadhi, and B.S. Sood, Phys. Rev. A **43**, 1455 (1991).
[40] K.S. Kahlon, N. Singh, R. Mittal, K.L. Allawadhi, and B.S. Sood, Phys. Rev. A **44**, 4379 (1991); *ibid.* **48**, 1701 (1993).
[41] J.K. Sharma and K.L. Allawadhi, J. Phys. B **32**, 2343 (1999).
[42] M. Ertuğrul, E. Büyükkasap, A. Küçükönder, A.I. Kopya, and H. Erdoğan, Nuovo Cimento D **17**, 993 (1995); M. Ertuğrul, E. Büyükkasap, and H. Erdoğan, *ibid.* **18**, 671 (1996).
[43] M. Ertuğrul, Nucl. Instrum. Methods Phys. Res. B **119**, 345 (1996).
[44] M. Ertuğrul and H. Erdoğan, Appl. Spectrosc. Rev. **32**, 159 (1997); M. Ertuğrul and E. Büyükkasap, *ibid.* **32**, 175 (1997).
[45] S. Seven and K. Koçak, J. Phys. B **34**, 2021 (2001).
[46] A. Kumar, S. Puri, D. Mehta, M.L. Garg, and N. Singh, J. Phys. B **32**, 3701 (1999).
[47] D. Mehta, S. Puri, N. Singh, M.L. Garg, and P.N. Trehan, Phys. Rev. A **59**, 2723 (1999); S. Puri, D. Mehta, J.S. Shahi, M.L. Garg, N. Singh, and P.N. Trehan, Nucl. Instrum. Methods Phys. Res. B **152**, 19 (1999).
[48] A. Kumar, S. Puri, J.S. Shahi, M.L. Garg, D. Mehta, and N. Singh, J. Phys. B **34**, 613 (2001); A. Kumar, M.L. Garg, S. Puri, D. Mehta, and N. Singh, X-Ray Spectrom. **30**, 287 (2001).
[49] T. Papp and J.L. Campbell, J. Phys. B **25**, 3765 (1992).
[50] V.V. Balashov, A.N. Grum-Grzhimailo, and N.M. Kabachnik, *Polarization and Correlation Phenomena in Atomic Collisions: A Practical Theory Course* (Kluwer/Plenum, New York, 2000), p. 159.
[51] J.H. Scofield, At. Data Nucl. Data Tables **14**, 121 (1974).
[52] U. Kleiman and B. Lohmann, J. Phys. B **33**, L641 (2000); U. Kleiman, *ibid.* **35**, 947 (2002).
[53] R.D. Cowan, *The Theory of Atomic Structure and Spectra* (University of California Press, Berkeley, CA, 1981).
[54] R.D. Cowan and D.C. Griffin, J. Opt. Soc. Am. **66**, 1010 (1976).
[55] N.M. Kabachnik and I.P. Sazhina, J. Phys. B **29**, L515 (1996).
[56] M. Ito, K. Hirano, M. Suzuki, E. Arakawa, S. Kishimoto, N. Kawamura, S. Maruyama and S. Goto, SPring-8 User Experiment Report No. 2, 1998, p. 159; H. Maruyama, M. Suzuki, N. Kawamura, M. Ito, E. Arakawa, J. Kokubun, K. Hirano, K. Horie, S. Uemura, K. Hagiwara, M. Mizumaki, S. Goto, H. Kitamura, K. Namikawa, and T. Ishikawa, J. Synchrotron Radiat. **6**, 1113 (1999).
[57] T. Papp, J.L. Campbell, and S. Raman, Phys. Rev. A **49**, 729 (1994); T. Papp, J.L. Campbell, D. Varga, and G. Kalinka, Nucl. Instrum. Methods Phys. Res. A **412**, 109 (1998).
[58] S. Goto, Nucl. Instrum. Methods Phys. Res. A **333**, 452 (1993); S. Goto, K. Sugishima, and Y. Ban, Radiat. Phys. Chem. **45**, 333 (1995); S. Goto, J. Synchrotron Radiat. **5**, 880 (1998).
[59] J.H. Hubbell and S.M. Seltzer, National Institute of Standards and Technology Report No. NISTIR 5632, 1995.
[60] Home page of the Center of X-RAY Optics, Lawrence Berkeley National Laboratory (URL: http://www-cxro. lbl. gov/optical_constants/).
[61] Expression (7) is written in the reference frame with z axis parallel to the electric-field vector. It differs by a factor of -2 from the corresponding expressions in Refs. [25,52] written in another reference frame with the z axis along the photon beam.